Measurements of decay branching fractions of the Higgs boson to hadronic final states at the CEPC

[1]Yanping Huang, [1]Xiaotian Ma, [1,2]Zuofei Wu, Shuo Han

[1]*Institute of High Energy Physics*

[2]*Nanjing University*

Contents

- Introduction
- Simulation samples
- Event selection
- Particle Transformer
- Model performance
- Measurements of branching fractions
- Summary

Introduction

- This study focuses on the precise determination of the branching fractions of $H \to b\bar{b}/c\bar{c}/gg/WW^*/ZZ^*/s\bar{s}$ in associated $Z(\mu^+\mu^-)H$ production at the CEPC with a center-of-mass energy of 240 GeV and integrated luminosity of 20 ab $^{-1}$.
- According to theoretical predictions, the branching fractions for the decay of a 125 GeV Higgs boson into $b\bar{b}$, $c\bar{c}$, gg, WW^*, ZZ^*, are 57.7%, 2.91%, 8.57%, 21.5%, 2.64%, respectively, and $s\bar{s}$ will also be considered. arXiv:1307.1347
- For WW^* and ZZ^*, the dominant decay modes are hadronic, making it challenging to distinguish them. And this can be overcome by end-to-end ML method.
- The Particle Transformer is applied to separate all decay channels simultaneously with high accuracy.

Sig	$H \to b\bar{b}$	$H \to c\bar{c}$	$H \to gg$	$H \to ZZ^*$	$H \to WW^*$	$H \to s\bar{s}$
predictions	57.7%	2.91%	8.57%	2.64%	21.5%	4.4×10^{-4}

Simulation samples

- Using Whizard 1.95 and Pythia6 for the fragmentation and hadronization
- Signal process: Z decays to a pair of muons and H decays in pairs of $b\bar{b}/c\bar{c}/gg/WW^*/ZZ^*/s\bar{s}$, full simulation generated under Ref-TDR CEPCSW
- Backgrounds: processes with two-fermion and four-fermion final states, fast detector simulation using a Delphes-based software

Signal process

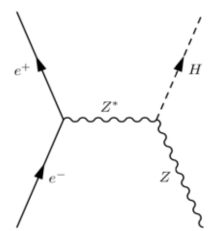

Process	Higgs decays	Cross section/fb
	$H \to b\bar{b}$	3.91
	$H \to c\bar{c}$	0.20
ZH process $Z \to \mu^+\mu^-$	$H \to gg$	0.58
	$H \to WW^*$	1.46
	$H \to ZZ^*$	0.18

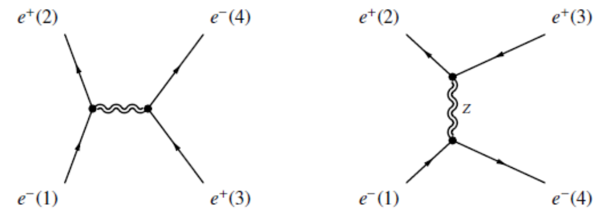

Two-fermion background process

Category	Name	Decay modes	Cross section/fb
Two-fermion background	$l\bar{l}$	$e^+e^- \to e^+e^-$	24992.21
		$e^+e^- \to \mu^+\mu^-$	4991.91
		$e^+e^- \to \tau^+\tau^-$	4432.18
	$\nu\bar{\nu}$	$e^+e^- \to \nu_e\bar{\nu}_e$	45390.79
		$e^+e^- \to \nu_\mu\bar{\nu}_\mu$	4416.30
		$e^+e^- \to \nu_\tau\bar{\nu}_\tau$	4410.26
	$q\bar{q}$	$e^+e^- \to u\bar{u}$	10110.43
		$e^+e^- \to d\bar{d}$	10010.07
		$e^+e^- \to c\bar{c}$	10102.75
		$e^+e^- \to s\bar{s}$	9924.40
		$e^+e^- \to b\bar{b}$	9957.70

- leptons (l), neutrinos (ν), and quarks (q)

Simulation samples

Four-fermion background process

➢ names refer to final states with leptons (l), hadrons (h), and semil eptons (sl).

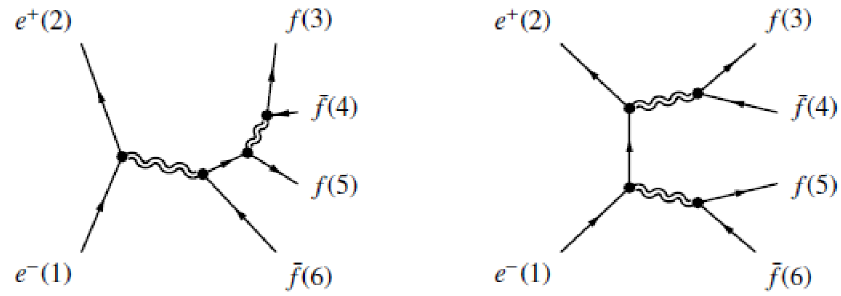

Four-fermion background	$(ZZ)_h$	$Z \to c\bar{c}, Z \to d\bar{d}/b\bar{b}$	98.97
		$ZZ \to d\bar{d}d\bar{d}$	233.46
		$ZZ \to u\bar{u}u\bar{u}$	85.68
		$Z \to u\bar{u}, Z \to s\bar{s}/b\bar{b}$	98.56
	$(ZZ)_l$	$Z \to \mu^+\mu^-, Z \to \mu^+\mu^-$	15.56
		$Z \to \tau^+\tau^-, Z \to \tau^+\tau^-$	4.61
		$Z \to \mu^+\mu^-, Z \to \nu_\mu\bar{\nu}_\mu$	19.38
		$Z \to \tau^+\tau^-, Z \to \mu^+\mu^-$	18.65
		$Z \to \tau^+\tau^-, Z \to \nu_\tau\bar{\nu}_\tau$	9.61
	$(ZZ)_{sl}$	$Z \to \mu^+\mu^-, Z \to d\bar{d}$	136.14
		$Z \to \mu^+\mu^-, Z \to u\bar{u}$	87.39
		$Z \to \nu\bar{\nu}, Z \to d\bar{d}$	139.71
		$Z \to \nu\bar{\nu}, Z \to u\bar{u}$	84.38
		$Z \to \tau^+\tau^-, Z \to d\bar{d}$	67.31
		$Z \to \tau^+\tau^-, Z \to u\bar{u}$	41.56
	$(WW)_h$	$WW \to uubd$	0.05
		$WW \to ccbs$	5.89
		$WW \to ccds$	170.18
		$WW \to cusd$	3478.89
		$WW \to uusd$	170.45

$(WW)_l$	$WW \to 4leptons$	403.66
$(WW)_{sl}$	$W \to \mu\bar{\nu}_\mu, W \to q\bar{q}$	2423.43
	$W \to \tau\bar{\nu}_\tau, W \to q\bar{q}$	2423.56
$(SZ)_l$	$e^+e^-, Z \to e^+e^-$	78.49
	$e^+e^-, Z \to \mu^+\mu^-$	845.81
	$e^+e^-, Z \to \nu\nu$	28.94
	$e^+e^-, Z \to \tau^+\tau^-$	147.28
	$\nu^+\nu^-, Z \to \mu^+\mu^-$	43.42
	$\nu^+\nu^-, Z \to \tau^+\tau^-$	14.57
$(SZ)_{sl}$	$e^+e^-, Z \to d\bar{d}$	125.83
	$e^+e^-, Z \to u\bar{u}$	190.21
	$\nu^+\nu^-, Z \to d\bar{d}$	90.03
	$\nu^+\nu^-, Z \to u\bar{u}$	55.59
$(SW)_l$	$e\nu_e, W \to \mu\nu_\mu$	436.70
	$e\nu_e, W \to \tau\nu_\tau$	435.93
$(SW)_{sl}$	$e\nu_e, W \to qq$	2612.62
$(mix)_h$	$ZZ/WW \to ccss$	1607.55
	$ZZ/WW \to uudd$	1610.32
$(mix)_l$	$ZZ/WW \to \mu\mu\nu_\mu\nu_\mu$	221.10
	$ZZ/WW \to \tau\tau\nu_\tau\nu_\tau$	211.18
	$SZ/SW \to ee\nu_e\nu_e$	249.48

Event selection

- At least two muons with opposite charge. (muon ID @ BEST WP and E > 10 GeV)
  - Choose the muon pair closest to the Z boson mass.
- Isolation cut: $E_{\text{cone}}^2 < 4E_\mu + 12.2\text{GeV}$
  - E_{cone} is the sum of energy within a cone ($\cos\theta_{cone} > 0.98$) around the muon.
- $M_{\mu\mu}$ in Z-mass window [75 GeV, 105 GeV].
- $M_{\mu\mu}^{\text{recoil}}$ in H-mass window [110 GeV, 150 GeV]. $M_{\mu\mu}^{\text{recoil}} = \sqrt{(\sqrt{s} - E_{\mu^+} - E_{\mu^-})^2 - (\overrightarrow{P_{\mu^+}} + \overrightarrow{P_{\mu^-}})^2}$
- $|\cos\theta_{\mu^+\mu^-}| < 0.996$: to further reduce the two-fermion backgrounds.
- $N_{\text{charged}} > 7$: to reduce the backgrounds.

The cutflow selection efficiency

Process	$H \to b\bar{b}$	$H \to c\bar{c}$	$H \to gg$	$H \to ZZ^*$	$H \to WW^*$	$H \to s\bar{s}$	$(ZZ)_{sl}$
Theo. N	78126	3940	11604	3575	29111	60	11129800
Simu. N	495000	494500	371500	497250	497000	494250	26499801
Muon pair	96.9%	96.7%	96.7%	96.7%	96.7%	96.6%	18.8%
Isolation	90.3%	90.3%	90.5%	90.7%	90.4%	90.5%	12.9%
Z-mass	86.7%	86.7%	86.9%	87.1%	86.8%	86.8%	9.1%
H-mass	86.4%	86.3%	86.5%	86.7%	86.4%	86.5%	1.5%
$\cos\theta$	86.1%	86.0%	86.2%	86.4%	86.1%	86.2%	1.5%
N_{charged}	86.1%	86.0%	86.2%	86.4%	86.1%	86.1%	1.5%

Event selection

- $M_{\mu\mu}$ and $M_{\mu\mu}^{\text{recoil}}$ distributions for signal and background events, following the muon pair and isolation selection criteria.

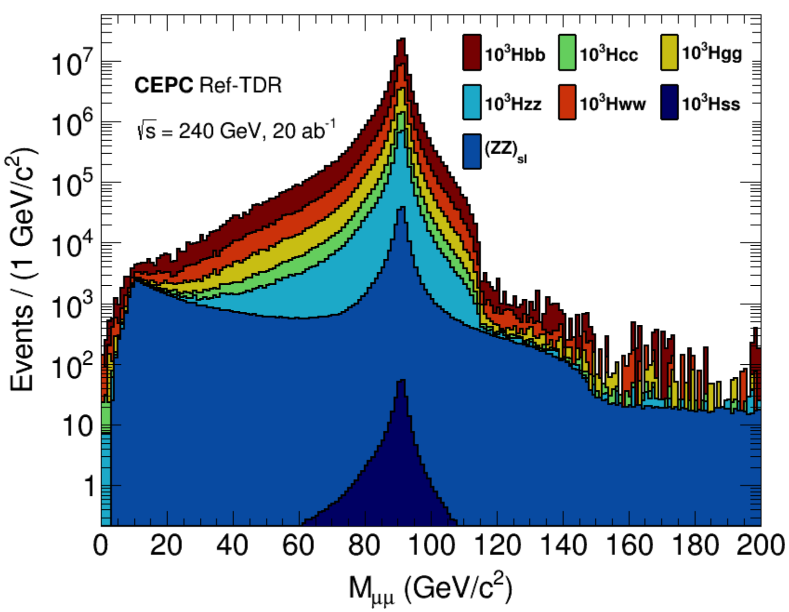

The invariant mass distributions of the muon pair

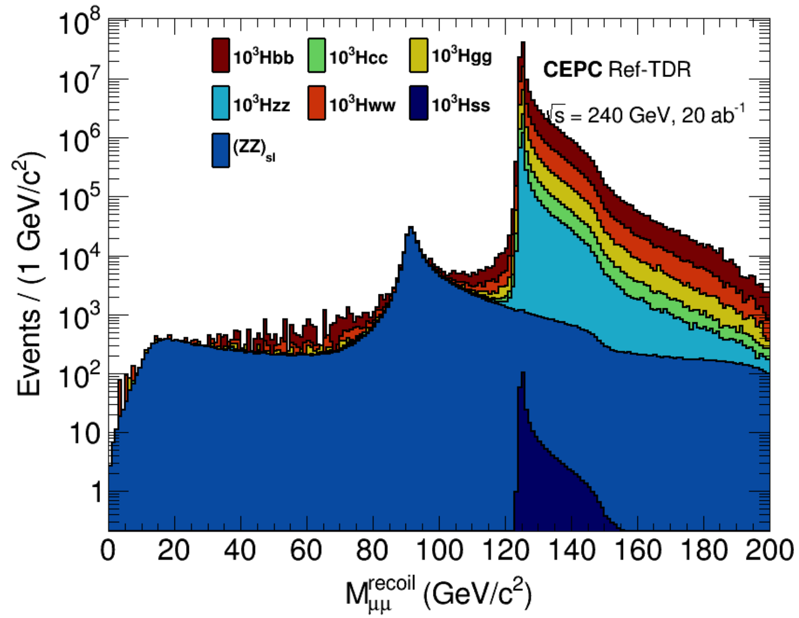

The invariant mass distributions of the muon pair recoil system

- The signal is well preserved while background contributions are significantly suppressed.

Particle Transformer

- A state-of-the-art deep learning model designed for particle physics.
- Transformer-Based architecture with particle feature embedding (edge) and class attention for jet-tagging and event classification…
- Advantages:
  - More training parameters and complicated architecture.
  - End-to-End learning which eliminates the dependency on jet clustering and e/γ isolation.
  - Effective edge information.

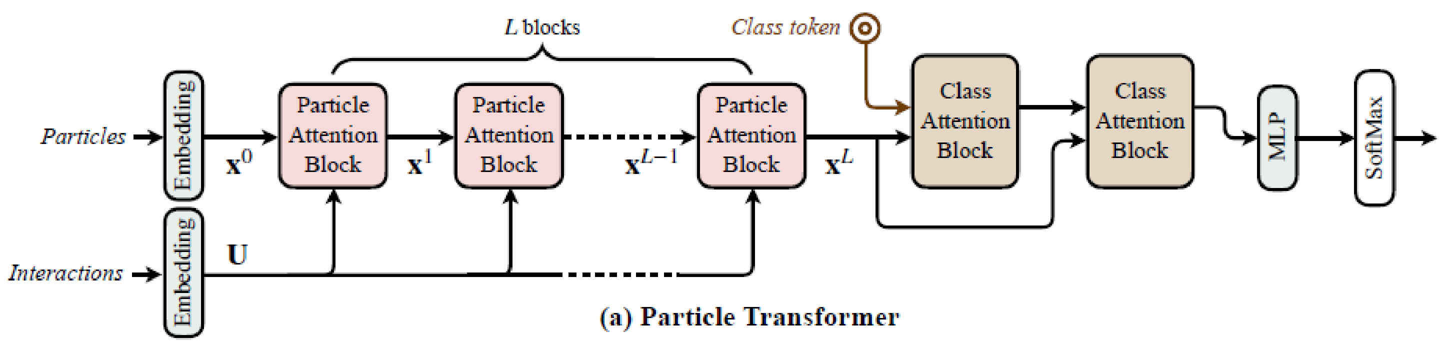

(a) Particle Transformer

The Particle Transformer architecture

Particle Transformer

- Samples：
  - 300k for each category, (training: validation: test sets) = (8:1:1)
  - Signal: $H \to b\bar{b}$、$H \to c\bar{c}$、$H \to gg$、$H \to ZZ^*$、$H \to WW^*$、$H \to s\bar{s}$ [full sim]
  - Background: $(ZZ)_{sl}$ [fast sim]

- Training variables：
  - Energy, momentum, cosθ, ϕ, PID, D_0, Z_0, charge, ZTag-> particle features.
  - Pt, eta, phi, E -> edge features.

- Training parameters：
  - Pair Embedding: (64, 64, 64, 16), Feature Embedding: (128, 512, 128).
  - 8 particle attention layers and 2 class attention layers with both 8 heads.
  - Fully connected layer: GeLU activation function and RAdam optimizer.
  - Epoch: 60, Learning rate: 0.001, Batchsize: 512

Model Performance

The migration matrix

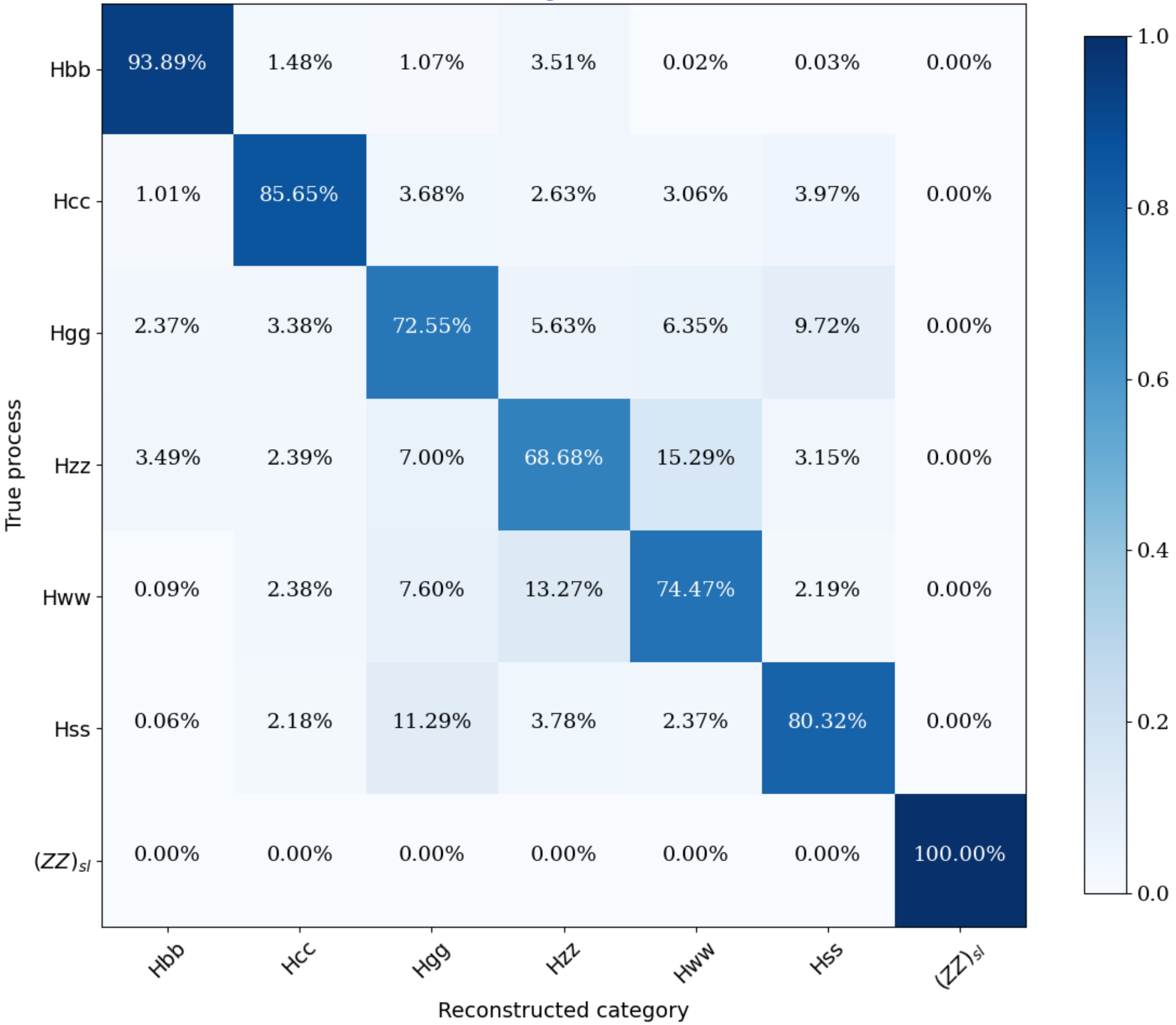

- The sum of each row equals 1
- Reconstructed category refers to one with maximum score
- Average accuracy: 82.2%

Model Performance

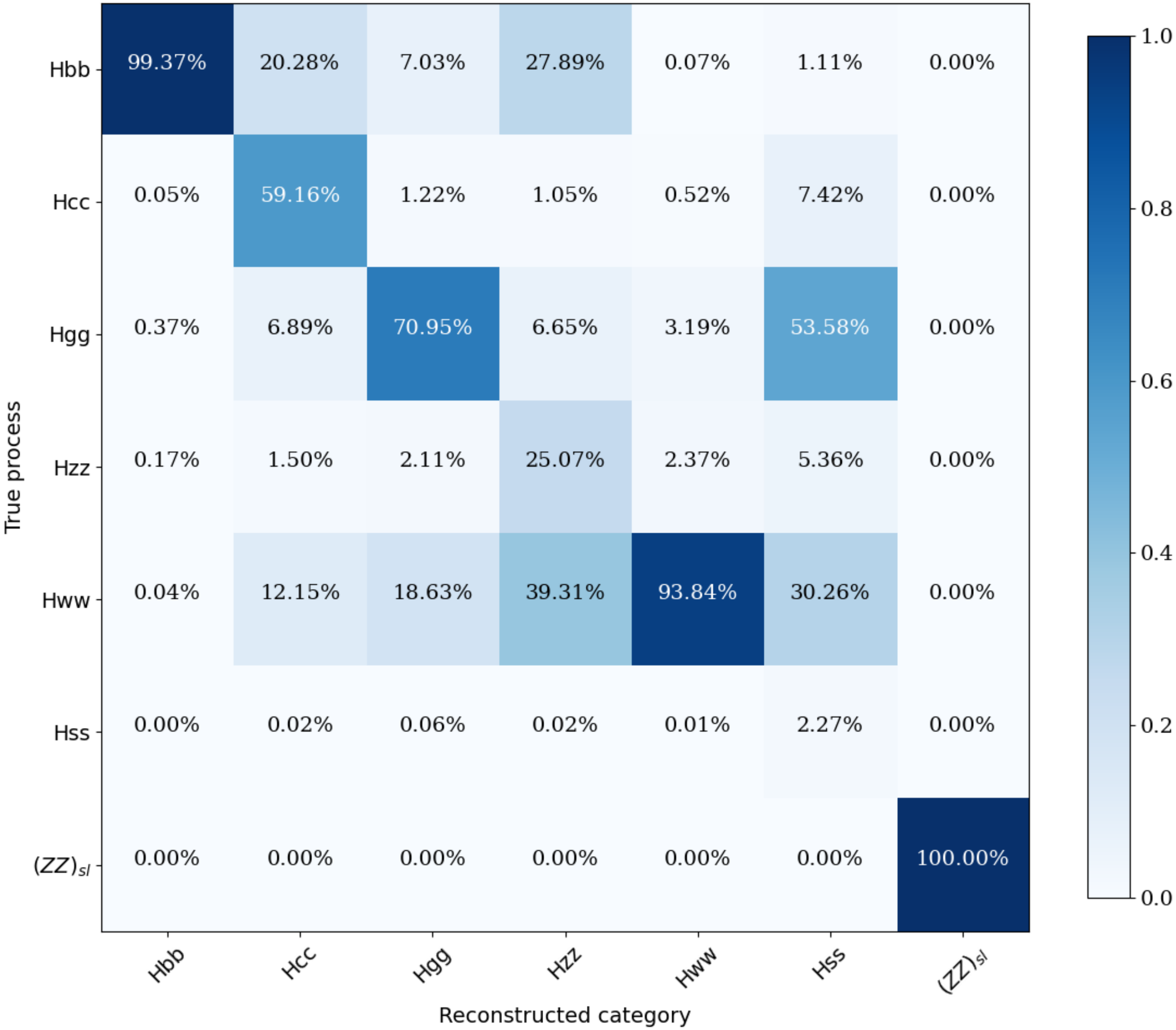

- Scaled to integrated luminosity
- The sum of each column equals 1
- Reconstructed category refers to one with maximum score
- For reconstructed $b\bar{b}$, 99% from truth $b\bar{b}$

Measurements of branching fractions

- Use the migration matrix method
  - Can be unfolded to represent the generated number of signals
  - Calculated as follows:

$$\begin{bmatrix} N_{s1} \\ N_{s2} \\ \cdots \\ N_{b1} \\ N_{b2} \\ \cdots \end{bmatrix} = \left(M_{mig}^T M_s\right)^{-1} \times \begin{bmatrix} n_{s1} \\ n_{s2} \\ \cdots \\ n_{b1} \\ n_{b2} \\ \cdots \end{bmatrix}$$

> - n_i and N_i: the expected and generated number of events of class i
> - M_s: a diagonal matrix containing the selection efficiencies
> - M_{mig}^T: the transposed migration matrix

- Use toyMC method to estimate statistical uncertainties
  - Sampling for 10k times according to Poisson distribution and Multinomial distribution
  - Minimize $\chi^2 = \Sigma_{i=0}^{6} \frac{(Y_i - \eta_i)^2}{\sigma_i^2}$ then fit with gaussian function

Statistical uncertainty

ToyMC test result

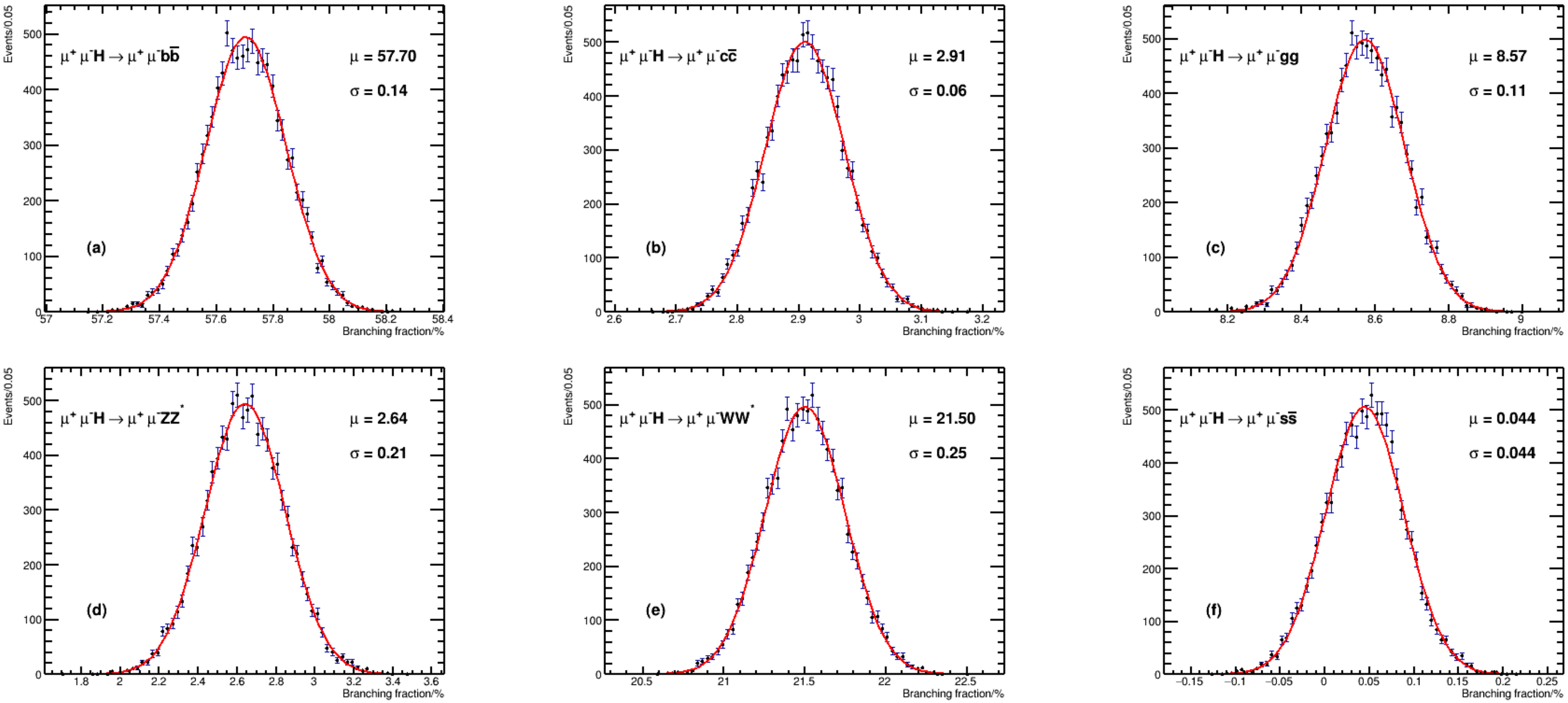

Sig	$H \to b\bar{b}$	$H \to c\bar{c}$	$H \to gg$	$H \to ZZ^*$	$H \to WW^*$	$H \to s\bar{s}$
Branching fraction	57.7%	2.91%	8.57%	2.64%	21.5%	4.4×10^{-4}
Rel. Stat. Un.	0.3%	2.2%	1.3%	7.8%	1.2%	98.8%

Systematic uncertainty

- To account for detector-related effects, particularly those arising from vertex reconstruction and tracking, the spatial resolution of each track was conservatively smeared from 5 μm to 10 μm.

- By applying the previous ML model to MC samples generated with updated resolutions, the differences in branching fractions before and after the resolution change are considered as the systematic uncertainty.

$$\sigma_{r\phi} = 5 \oplus \frac{10}{p(\mathrm{GeV}) \sin^{3/2}\theta} \mu\mathrm{m}. \xrightarrow{\text{smear}} \sigma_{r\phi} = 10 \oplus \frac{10}{p(\mathrm{GeV}) \sin^{3/2}\theta} \mu\mathrm{m}.$$

Sig	$H \to b\bar{b}$	$H \to c\bar{c}$	$H \to gg$	$H \to ZZ^*$	$H \to WW^*$	$H \to s\bar{s}$
Branching fraction	57.7%	2.91%	8.57%	2.64%	21.5%	4.4×10^{-4}
Rel. Syst. Un.	0.1%	6.6%	5.1%	13.2%	2.0%	451.8%

Results

- Results of the measured Higgs branching fractions with relative statistical and systematic uncertainties:

Sig	$H \to b\bar{b}$	$H \to c\bar{c}$	$H \to gg$	$H \to ZZ^*$	$H \to WW^*$	$H \to s\bar{s}$
Branching fraction	57.7%	2.91%	8.57%	2.64%	21.5%	4.4×10^{-4}
Rel. Stat. Un.	0.3%	2.2%	1.3%	7.8%	1.2%	98.8%
Rel. Syst. Un.	0.1%	6.6%	5.1%	13.2%	2.0%	451.8%

Summary

- The Higgs boson branching fractions into $b\bar{b}/c\bar{c}/g\bar{g}/s\bar{s}$ and WW^*/ZZ^*, where the W or Z bosons decay hadronically, via the $Z(\mu^+\mu^-)H$ process are studied using the Particle Transformer method at a center-of-mass energy of 240 GeV and a luminosity of 20 ab $^{-1}$ at the CEPC.

- The relative statistical uncertainties of branching fractions of $H \to b\bar{b}/c\bar{c}/gg/WW^*/ZZ^*/s\bar{s}$ processes are estimated to be 0.3%, 2.2%, 1.3%, 7.8%, 1.2% and 98.8%, respectively.

- To account for detector-related effects, particularly those arising from vertex reconstruction and tracking, the spatial resolution of each track was conservatively smeared from 5 μm to 10 μm, and the relative systematic uncertainties are estimated to be 0.1%, 6.6%, 5.1%, 13.2%, 2.0% and 451.8%, respectively.

Back up

Systematic uncertainty

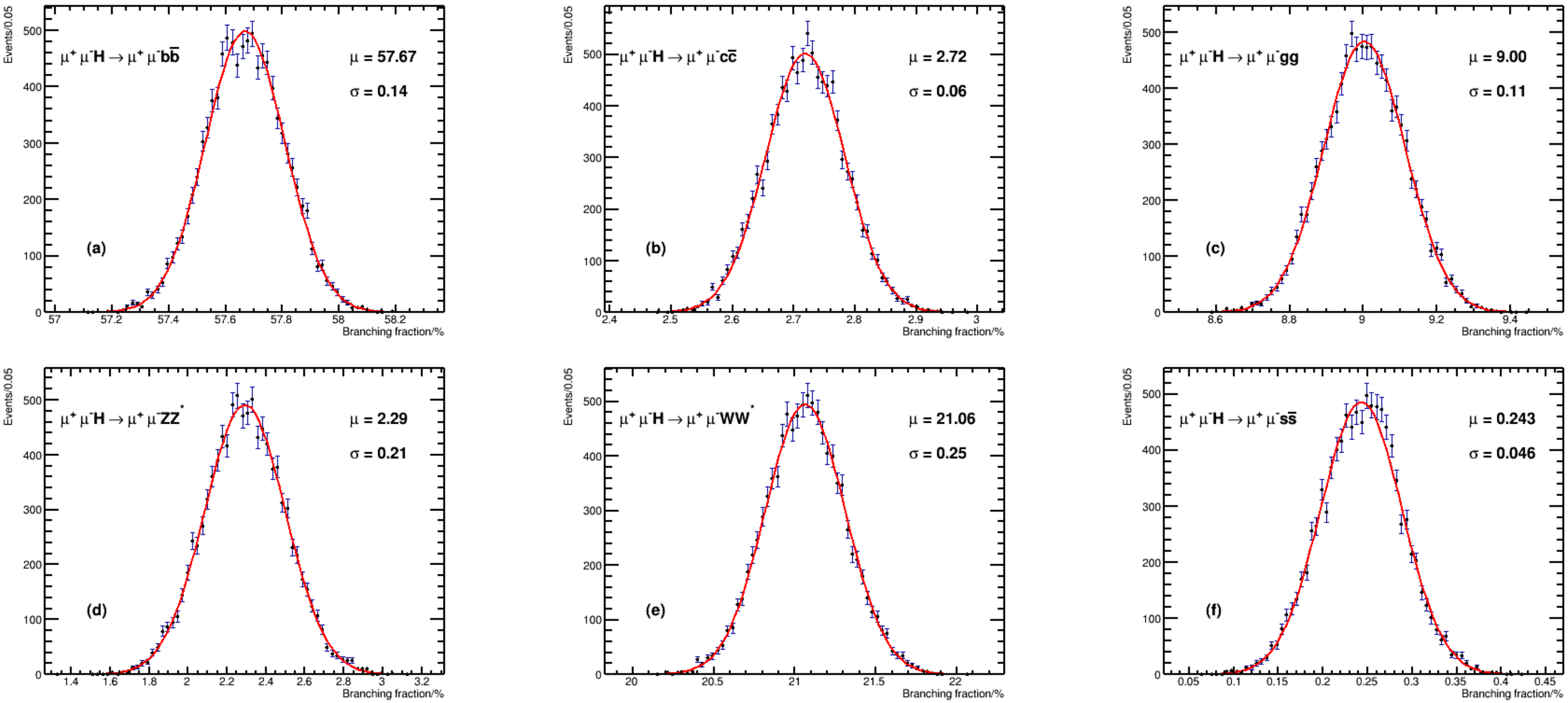

Sig	$H \to b\bar{b}$	$H \to c\bar{c}$	$H \to gg$	$H \to ZZ^*$	$H \to WW^*$	$H \to s\bar{s}$
Branching fraction	57.7%	2.91%	8.57%	2.64%	21.5%	4.4×10^{-4}
Rel. Syst. Un.	0.1%	6.6%	5.1%	13.2%	2.0%	451.8%

Systematic uncertainty

$$\sigma_{r\phi} = 5 \oplus \frac{10}{p(\mathrm{GeV})\sin^{3/2}\theta}\,\mu\mathrm{m}.$$

smear

$$\sigma_{r\phi} = 10 \oplus \frac{10}{p(\mathrm{GeV})\sin^{3/2}\theta}\,\mu\mathrm{m}.$$

The sum of each row equals 1

After smear

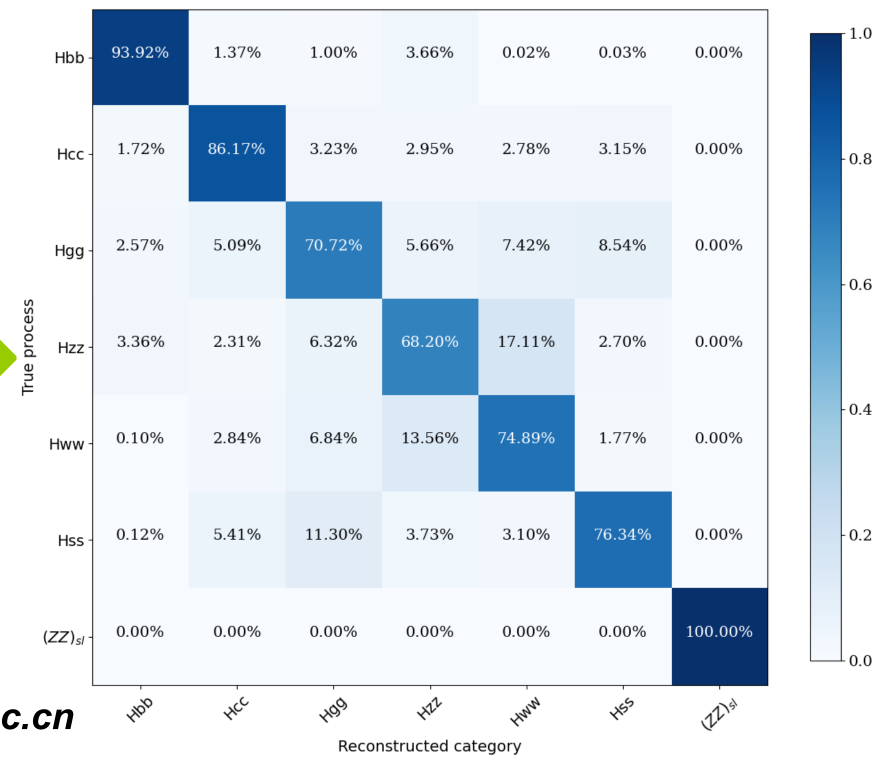

maxt@ihep.ac.cn

Systematic uncertainty

The sum of each column equals 1

After smear

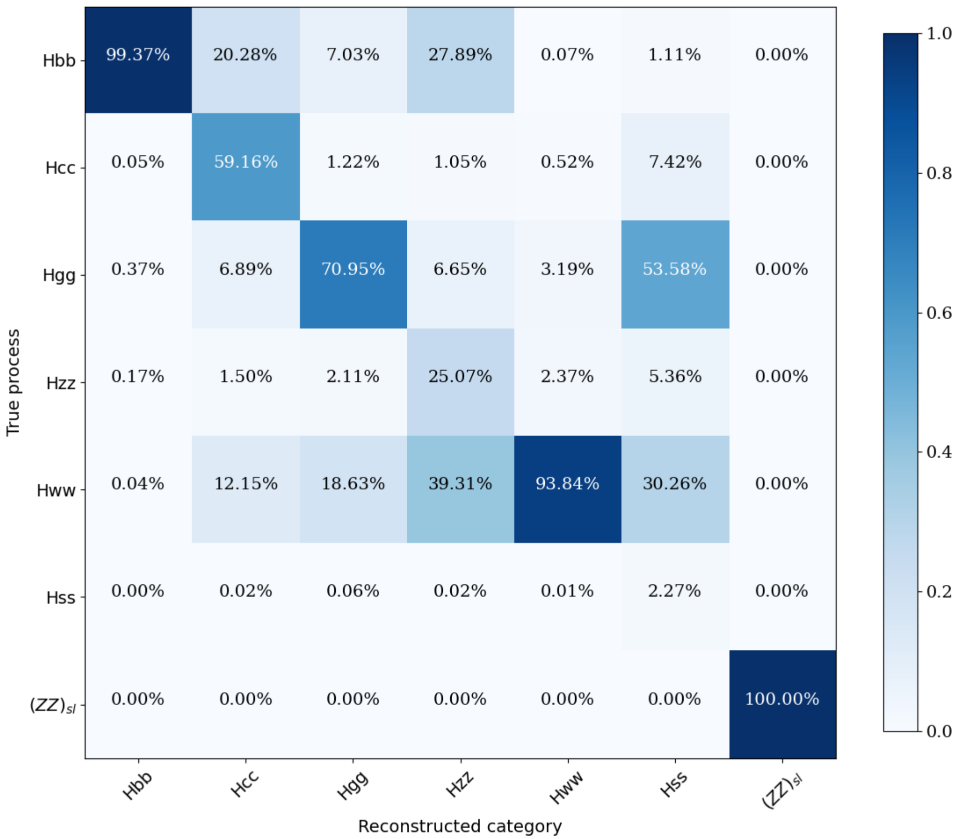

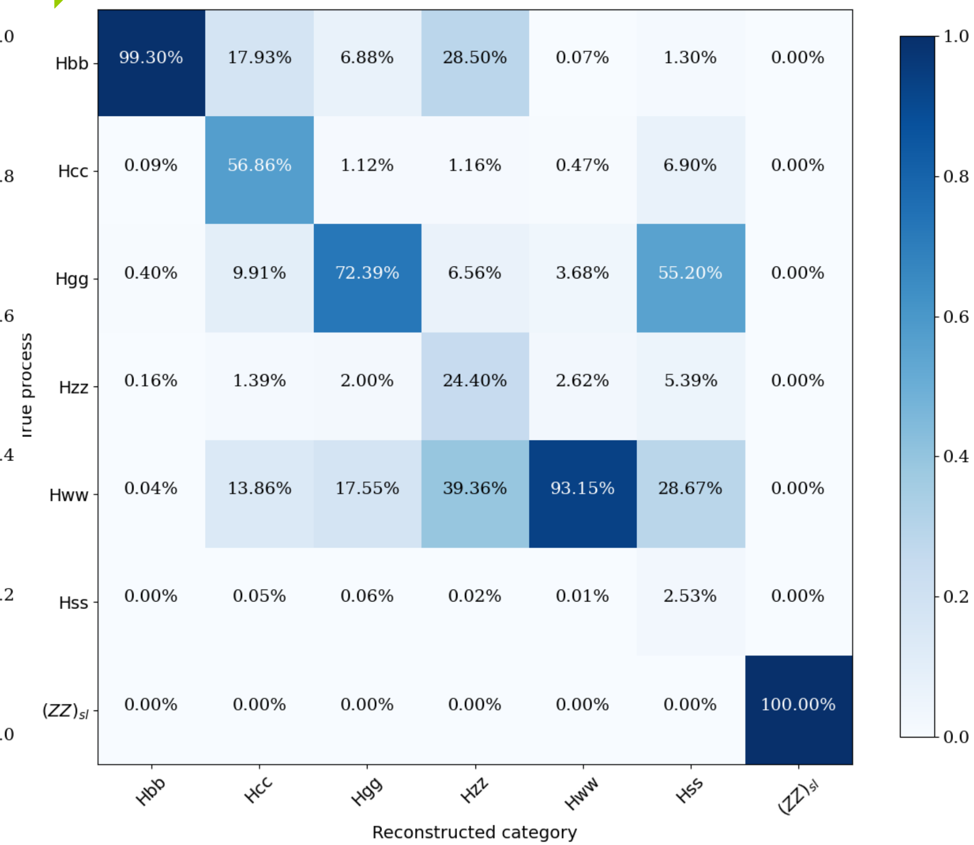

Distributions of signal vs bkg

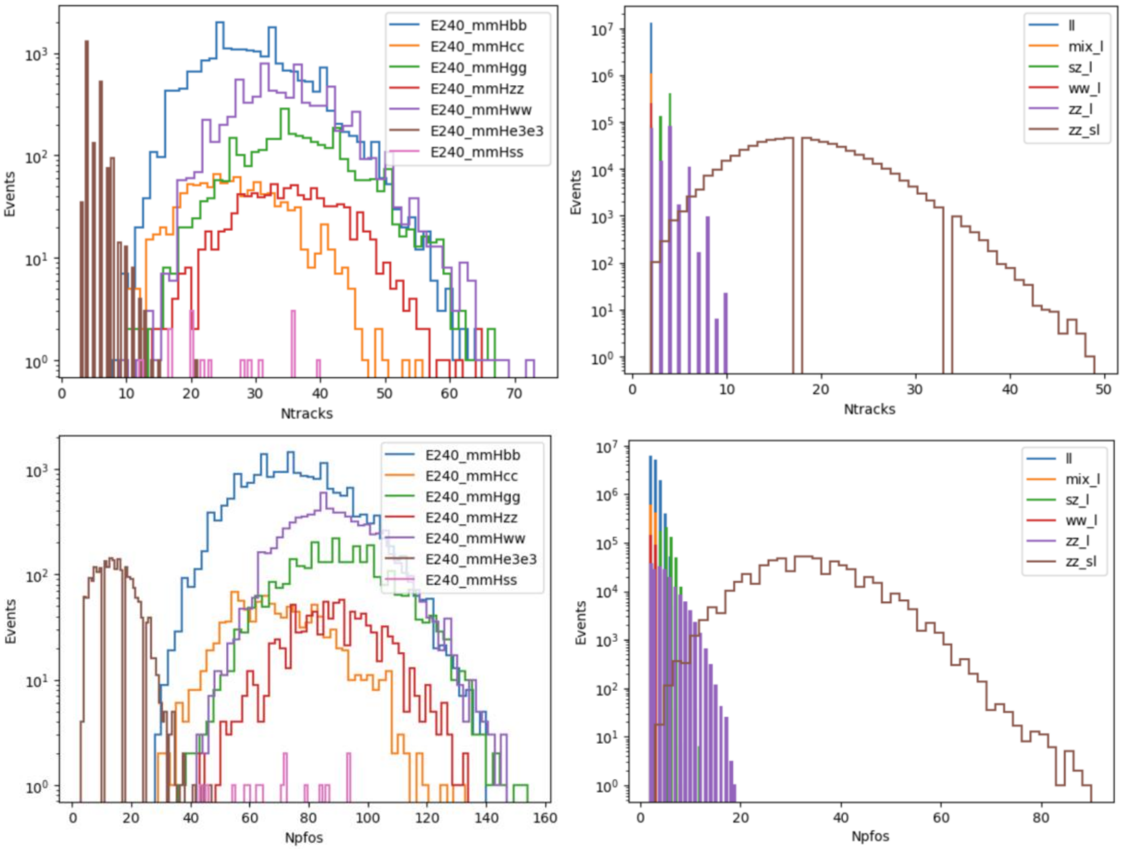

in signal

in bkg

Distributions of signal vs bkg

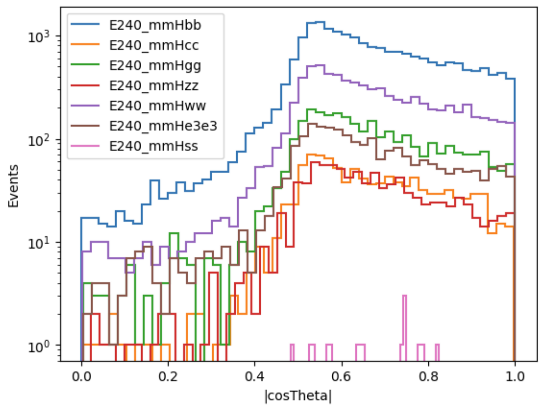

$|\cos\theta|$ distributions in signal

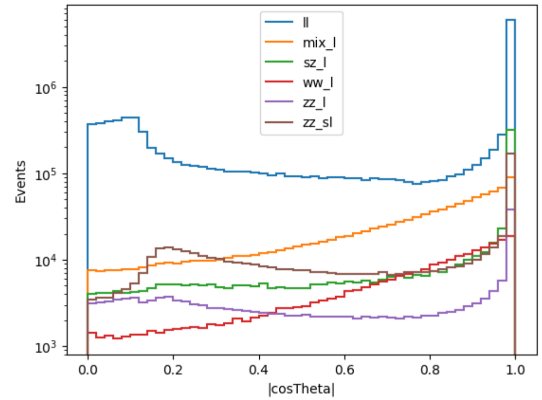

$|\cos\theta|$ distributions in background

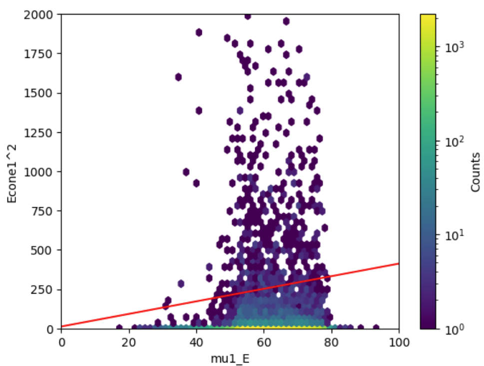

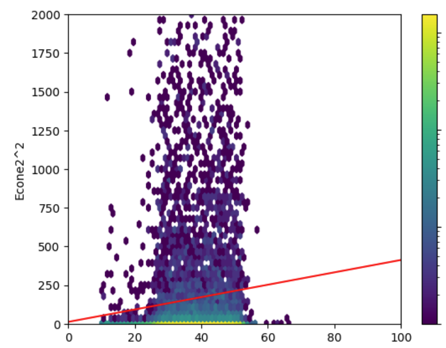

signal

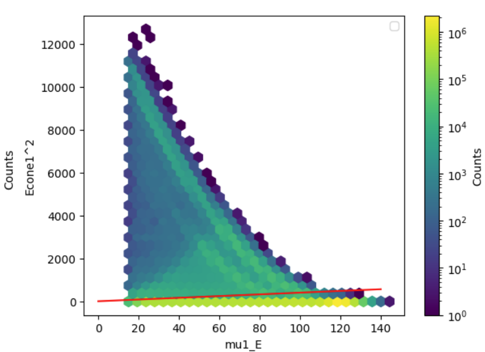

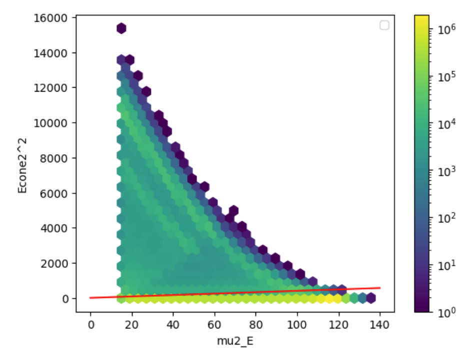

background

E_{cone}^2 vs E_μ in muon pairs.

Mass distributions

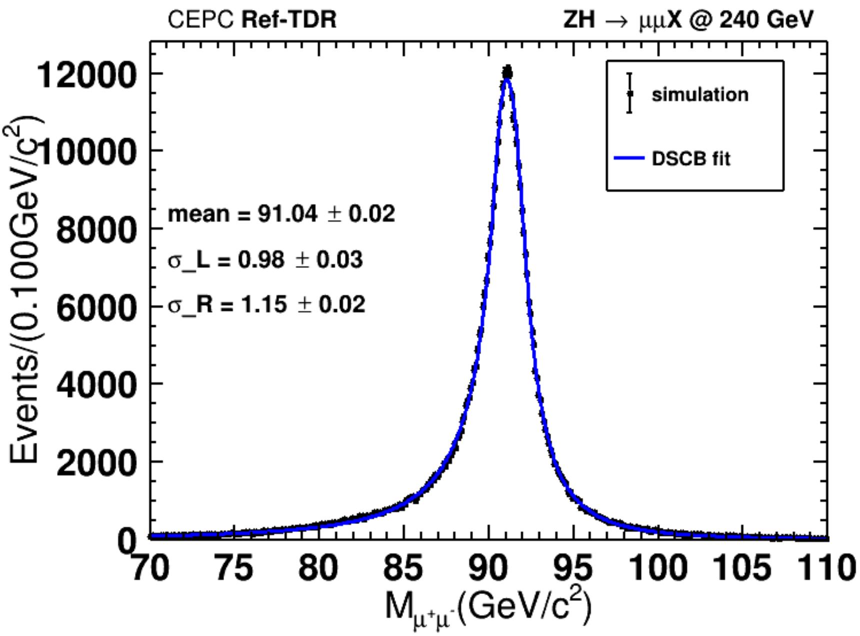

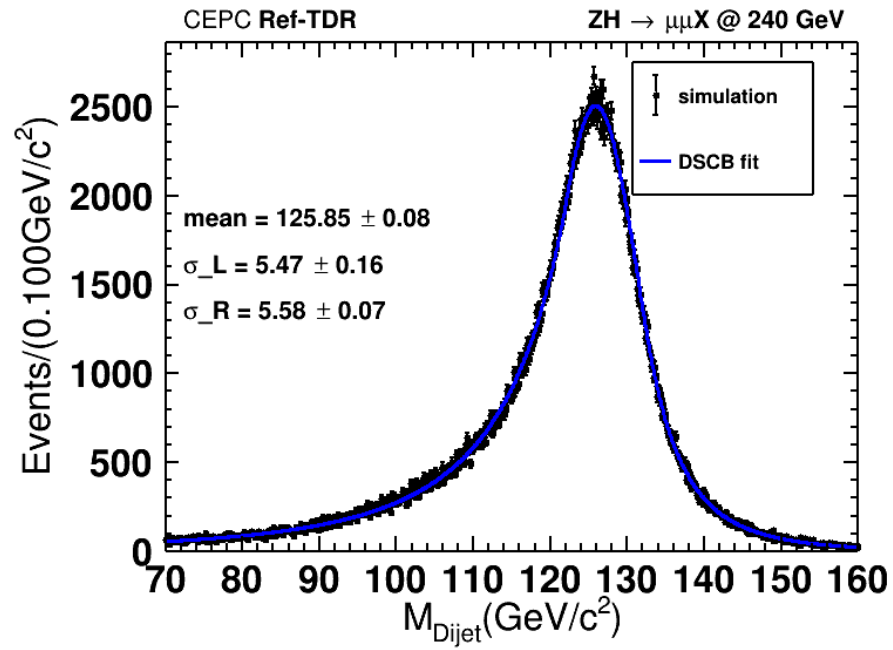

eekt jet clustering after removing muons in Z

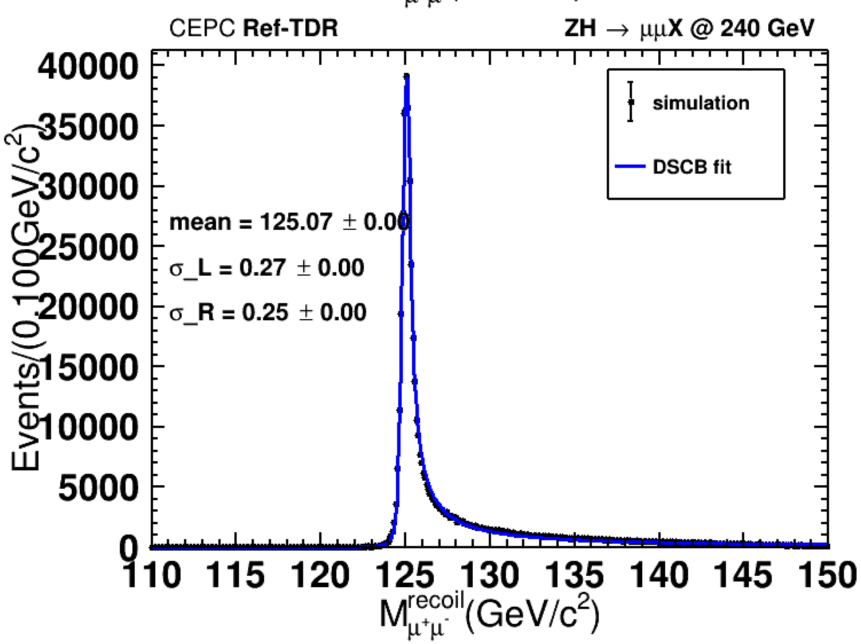

13-classification results

Table 15.6: The cutflow selection efficiency for signal processes.

Process	$b\bar{b}$	$c\bar{c}$	gg	$\tau\bar{\tau}$	WW^*	ZZ^*	$s\bar{s}$
Muon pair	93.4%	93.1%	92.9%	94.3%	93.0%	93.1%	93.2%
Isolation	93.0%	93.3%	93.7%	94.6%	93.6%	93.8%	93.5%
Z mass window	96.1%	96.1%	96.1%	93.2%	96.0%	96.0%	96.0%
H mass window	99.6%	99.6%	99.6%	98.5%	99.6%	99.6%	99.6%
$\lvert\cos\theta_{\mu\mu}\rvert$ <0.996	99.6%	99.7%	99.6%	99.7%	99.6%	99.7%	99.7%
Total eff.	82.8%	82.9%	83.0%	81.6%	82.9%	83.2%	83.0%

Table 15.7: The cutflow selection efficiency for background processes.

Process	$(ZZ)_l$	$(ZZ)_{sl}$	$(WW)_l$	ll	$(SZ)_l$	$(mix)_l$
Muon pair	46.1%	18.8%	11.0%	11.9%	9.7%	29.3%
Isolation	77.4%	68.8%	98.0%	94.6%	48.2%	96.1%
Z mass window	66.4%	70.4%	34.7%	41.8%	28.3%	16.8%
H mass window	15.6%	16.3%	58.6%	6.6%	29.3%	41.1%
$\lvert\cos\theta_{\mu\mu}\rvert$ <0.996	98.8%	99.5%	98.7%	90.3%	99.0%	99.4%
Total eff.	3.7%	1.5%	2.2%	0.3%	0.4%	1.9%

Relative efficiency and total efficiency for each survived channel

13-classification results

Decay channels	$b\bar{b}$	$c\bar{c}$	gg	$\tau\bar{\tau}$	WW^*	ZZ^*
BR	57.7%	2.9%	8.6%	6.3%	21.5%	2.6%
Rel. Stat. Un.	0.4%	6.7%	2.4%	1.2%	1.5%	18.6%
Rel. Syst. Un.	0.3%	24.8%	5.0%	0.04%	1.5%	66.0%

The branching fraction of $H \to s\bar{s}$ is measured to be <1.2% @ 95% CL.